Preparation and chiroptical properties of cellulose chlorophenylcarbamate–silica hybrids having a chiral nematic mesomorphic structure

Junichi Sato [a], Kazuki Sugimura [a], Yoshikuni Teramoto [b], and Yoshiyuki Nishio [a]*

[a] *Division of Forest and Biomaterials Science, Graduate School of Agriculture, Kyoto University, Sakyo-ku, Kyoto 606-8502, Japan*

[b] *Faculty of Applied Biological Sciences, Gifu University, 1-1 Yanagimoto, Gifu 501-1193, Japan*

*To whom correspondence should be addressed.

E-mail: ynishio@kais.kyoto-u.ac.jp. Phone: +81 75 753 6252. Fax: +81 75 753 6300.

ABSTRACT: An attempt was made to fabricate optically functional cellulosic–silica hybrid materials wherein a helically ordered mesomorphic structure of the cellulosic component was fixed. Cellulose 3-chlorophenylcarbamate (3Cl-CPC) and cellulose 4-chlorophenylcarbamate (4Cl-CPC) were synthesized by carbanilating reaction of cellulose with 3-chlorophenyl or 4-chlorophenyl isocyanate in a homogeneous solution system. The hydrophobic cellulose derivatives were examined for the solubility and liquid crystallinity in various solvents containing alkoxysilane as a main component. Concentrated (~40 wt%) solutions of 3Cl-CPC in 3-aminopropyltrimethoxysilane (APTMS) and those of 4Cl-CPC in a mixed solvent of tetramethoxysilane (TMOS)/*N*,*N*-dimethylformamide (DMF)/dichloroacetic acid (DCA) formed a chiral nematic mesophase to impart vivid reflection colors. These liquid crystalline solutions were subjected to a sol–gel conversion process of the respective alkoxysilane components in moist air. In the process for the 4Cl-CPC lyotropic system, we utilized a "surface-coating solvent" consisting of TMOS/phenyltrimethoxysilane/DCA to facilitate the sol–gel reaction of TMOS and also to preserve the reflective coloration. Thereby a left-handed chiral nematic hybrid series of 4Cl-CPC–silica was successfully obtained as a monolithic glassy bulk showing iridescent colors. The 3Cl-CPC/APTMS lyotropics were readily converted into a colored solid form without any coating solution, resulting in production of a right-handed chiral nematic series of 3Cl-CPC–silica. Besides investigating the chiroptical characteristics of the liquid crystalline solutions and hybrids, we preliminarily tried separating a racemic compound into two enantiomers by open column chromatography using the cellulosic–silica hybrids as a filler material of the column.

Keywords: Cellulose phenylcarbamate derivatives, Chiral nematic liquid crystals, Silica hybrids

1. Introduction

Cellulose derivatives as macromolecules and also cellulose nanocrystals (CNCs) as fragmented microfibrils can form a liquid-crystalline phase in solutions or suspensions with a suitable solvent under adequate conditions [1–7]. The mesogenic assembly structure in the anisotropic phase is usually chiral nematic (synonymous with cholesteric here). This supramolecular structure is characterized by the director of nematic orientation that propagates rotationally along one direction to make a left-handed or right-handed helical arrangement of pitch P (see Fig. 1). When the value of P is comparable to wavelengths (λ) of visible light, the formed chiral nematic mesophase imparts a color due to λ-selective light reflection. In addition, the reflective light is circularly polarized in a left-handed or right-handed manner, and this handedness of circularity coincides with the handedness of the chiral nematic helical arrangement considered.

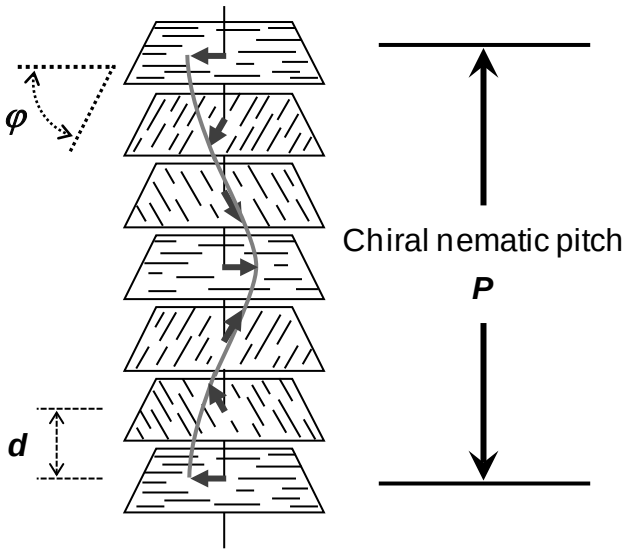

Fig. 1. Schematic illustration of the chiral nematic mesophase with a left-handed helical arrangement of mesogenic molecules. (A mirror image of this illustration corresponds to the right-handed chiral nematic arrangement.) The nematic layer spacing d and twist angle φ are defined so that they satisfy a relation $\varphi/d = 360°/P$ with the chiral nematic pitch P.

The chiral mesomorphic order in the cellulosics' lyotropics can be carried over into solid composites, typically by polymerizing reactive monomers as the solvent component [8–10]; thereby, we can design and fabricate colorful optical films whose coloration varies with the polymer composition and will be changeable by some external forces [7,10]. In the recent stream, inorganics such as calcic biominerals and ceramic silica, rather than organic polymers only, are involved in the compositions for acquiring additional thermomechanical performances or other functionalities. Such a novel class of cellulosic composites is

attainable, for example, by deposition of calcium phosphate or carbonate in nanosize onto the cellulosics-derived chiral nematic stratums [11,12], and also by formation of silica networks using a similar liquid-crystalline organization as template [13,14].

Concerning the silica hybridizations, an earlier report by the Mann's group [15] dealt with a CNC–silica hybrid composite obtained via the so-called sol–gel conversion process (Scheme 1) [16–18] of tetramethoxysilane (TMOS), this alkoxysilane being used as a solvent component of liquid-crystalline aqueous CNC suspensions. A contemporary report by Thomas and Antonietti [19] included an iridescently colored hybrid material of hydroxypropyl cellulose (HPC)–silica, which was also produced by the sol–gel process of TMOS as a solvent component of aqueous lyotropics of HPC. Both the cellulosic–silica hybrids were further transformed into net silica glasses retaining a chiral nematic pore structure by post-treatment of calcination to remove the CNC and HPC templates. More recently, MacLachlan, Hamad, and their coworkers synthesized a wide variety of iridescent mesoporous silicas using a chiral nematic CNC liquid-crystalline template for development of photonic and electronic materials [14,20,21], where diverse functionalities were assigned to the optically chiral silicas by loading relevant guest substances into the mesopores. Attention should be drawn, however, to the fact that all the materials based on CNC chiral mesomorphy shared a common feature of preserving the inherent left-handed helical structure [22,23]. Incidentally, the chiral nematics of HPC and its ester/ether derivatives are commonly in a right-handed helical fashion [2,4,7].

Hydrolysis:

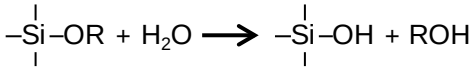

Polycondensation:

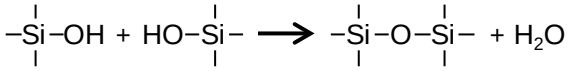

Scheme 1. Two successive reactions, hydrolysis and polycondensation, comprising the sol–gel process of alkoxysilane (e.g. TMOS with R = CH_3).

In the above examples demonstrating cellulosics–silica hybridizations, the mesogenic cellulosics, CNC and HPC, are both hydrophilic, and thus the sol–gel process of alkoxysilane for imprinting the chiral nematic structure was applied to completely aqueous lyotropic systems. Generally, the conversion process is made up of the successive hydrolysis and polycondensation of alkoxysilane (see Scheme 1) and can easily go in aqueous media [17,18].

In the present work, cellulose phenylcarbamate (CPC) derivatives of hydrophobic nature were employed as the mesogen component. Efforts were made to prepare the chiral nematic liquid-crystalline solutions using a suitable alkoxysilane for the main solvent and to immobilize the helically arranged structure into silica glasses by adapting the sol–gel method to the rather hydrophobic system.

With regard to the CPC family, it is known that a small difference in chemical modification of the aromatic substituent strongly influences the solubility in solvents and even the chiral nematic twist of the liquid crystals [3,4]. In this work, cellulose 3-chlorophenylcarbamate (3Cl-CPC) and cellulose 4-chlorophenylcarbamate (4Cl-CPC) (see Fig. 2a) were chosen and synthesized as a comparable pair of CPC derivatives. This choice for samples is based on the existing result [24]: High-substituted CPC and 4Cl-CPC formed a left-handed chiral nematic mesophase in diethylene (or triethylene) glycol monomethyl ether, whereas 3Cl-CPC formed a right-handed mesophase in the same solvents. By deduction from the result, we can expect a similar inversion in the twist handedness between 3Cl-CPC and 4Cl-CPC chiral nematics with other solvents involving alkoxides of Si. In addition, the CPC family is known to possess a chiral resolution power for enantiomers [25], and, actually, some derivatives are coated onto silica gels and used as fillers for a chiral column of high performance liquid chromatography (HPLC) [25–27], where it is suggested that a helical structure of the polysaccharide molecules makes a suitable spatial condition for the chiral separation. Therefore, the targeted CPC derivatives–silica hybrids may be of significance for demonstration of a dual-purpose functional material that separates light waves and even chiral substances (optical isomers). In this context, the present paper includes a preliminary chromatographic test for enantiomer separation using the prepared hybrids as column fillers, besides detailed characterization of their chiroptical properties derived from the CPCs' mesomorphy.

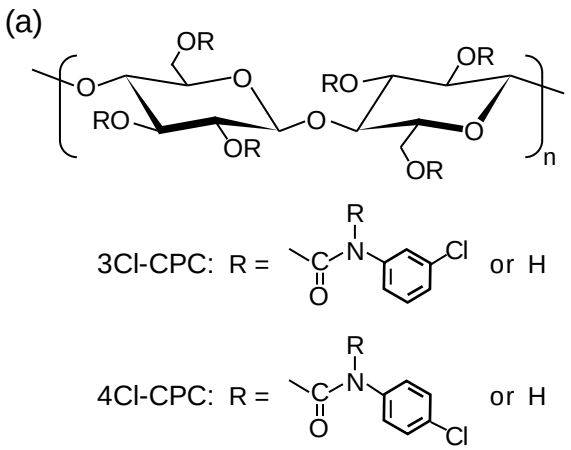

(b)

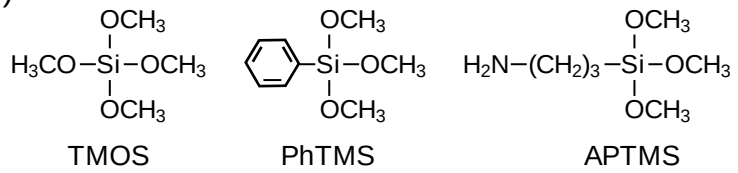

Fig. 2. Structural formulae of (a) cellulosic derivatives, 3Cl-CPC and 4Cl-CPC, and (b) alkoxysilanes, TMOS, PhTMS, and APTMS.

2. Experimental

2.1. Original materials

Microcrystalline cellulose Avicel® (hereinafter Avicel) was purchased from Merck KGaA, Germany and used after drying at 100 °C. The weight-average degree of polymerization of this cellulose has been estimated at ~525 by GPC analysis in the form of propionyl derivative [28]. Phenyl isocyanate (PhI), 3-chlorophenyl isocyanate (3ClPhI), and 4-chlorophenyl isocyanate (4ClPhI) were purchased from Wako Pure Chemical Ind., Ltd. and used as received. *N*,*N*-Dimethylacetamide (DMAc) (dehydrated) and lithium chloride (LiCl) (anhydrous) were products of Wako Pure Chemical Ind., Ltd. and Nacalai Tesque, Inc., respectively, and used for making the solvent system DMAc-LiCl to dissolve cellulose and synthesize its carbanilate derivatives.

Various alkoxysilanes, TMOS, phenyltrimethoxysilane (PhTMS), 3-aminopropyltrimethoxysilane (APTMS), methyltrimethoxysilane (MTMS), diphenyldimethoxysilane (DPhDMS), and dimethyldimethoxysilane (DMDMS), were purchased from Tokyo Kasei Kogyo Co., Ltd. and used as received. TMOS, PhTMS, and APTMS (see Fig. 2b) of the alkoxysilanes were chiefly utilized for forming the silica to hybridize with the target CPC derivatives. *N*,*N*-Dimethylformamide (DMF), dichloroacetic acid (DCA), and other chemicals were purchased from Wako Pure Chemical Ind., Ltd. or Nacalai Tesque, Inc.; all were guaranteed reagent-grade and used without further purification.

2.2. Synthesis of Cellulose Chlorophenylcarabamates, 3Cl-CPC and 4Cl-CPC

A homogeneous solution of cellulose in DMAc-LiCl (salt conc., 7.0 wt%) was prepared, typically as follows. Avicel cellulose (4.5 g) and DMAc (145 g) were put in a flask and the mixture was stirred at 130 °C for 1.5 h under a nitrogen atmosphere. Then the mixture (suspension) was cooled to 100 °C and LiCl powder (11 g) was added thereto. After 15 min stirring at this temperature, the mixture was gradually cooled to transform into a clear solution of 2.8 wt% cellulose. Complete dissolution of cellulose was confirmed using a polarized

optical microscope.

The isocyanate reagent 3ClPhI or 4ClPhI (7.5–10 mol equiv per anhydroglucose unit (AGU) of cellulose) was added to the cellulose solution mentioned above, and the reactive system was continuously stirred at 25 °C or 60 °C under a nitrogen atmosphere. After reaction over a prescribed time period (48–120 h), the solution was added dropwise to a vigorously stirred, excess amount of distilled water/methanol (1:1, v/v). Each product (3Cl-CPC or 4Cl-CPC) obtained as a precipitate was filtered and purified by dissolution–reprecipitation with DMF and distilled water/methanol. The purified 3Cl-CPC and 4Cl-CPC samples were each treated by a Soxhlet extraction with methanol for 72 h to remove DMF thoroughly, then dried at 40 °C for 48 h in a vacuum oven. In a similar way using non-chlorinated PhI as the attacking reagent, a mere CPC sample was synthesized as a reference standard. These preparation conditions were decided by reference to those applied to carbanilation of chitinous polysaccharides [29–31].

2.3. Preparation of 3Cl-CPC and 4Cl-CPC lyotropics

3Cl-CPC solutions were prepared in a polymer concentration range of 32–40 wt% by using APTMS for the solvent. The prescribed amount of APTMS was added to 3Cl-CPC powder weighed in a hermetically sealable glass vial and placed at 20 °C over a period of more than 1 week. In the procedure, the vial was turned upside down and centrifuged at intervals for the purpose of accelerating the dissolution of 3Cl-CPC. On the other hand, 4Cl-CPC solutions (32–48 wt%) were prepared by using a mixed solvent consisting of TMOS/DMF/DCA (6:3:2 in weight ratio), in a similar way of polymer dissolution. The selection of these solvents was made on the basis of the observations of polymer solubility and liquid crystallinity with available alkoxysilanes and organics (see Sect. *3.1.2*), and also by taking into consideration the facility of sol–gel processing for the given lyotropic system.

2.4. Preparation of hybrid samples, 3Cl-CPC–silica and 4Cl-CPC–silica

Liquid crystalline 3Cl-CPC/APTMS solutions, each matured at >35 wt% in a light-blocked glass vial, were exposed to the air conditioned at 25 °C and 50 % RH by taking off the top of the sample vial. The quiescent standing as that for 1 week enabled the initially fluid solution to gelate and solidify into a 3Cl-CPC–silica hybrid in a bulky cylindrical form.

With regard to 4Cl-CPC solutions in TMOS/DMF/DCA, such a simple casting technique allowing their immediate contact with moist air was not applicable to produce 4Cl-CPC–silica hybrids; because this lyotropic series readily whitened due to segregation of 4Cl-CPC in the sol–gel reaction process of TMOS that absorbed an excess amount of water. Therefore, an

alternative method using a coating solvent, TMOS/PhTMS/DCA (1:1:1 mixture in weight), was adopted for the hybrid preparations (see Sect. *3.3.1* for details of the advantage). In this method, first, the upper surface area of each liquid-crystalline sample matured at ≥40 wt% in a glass vial was covered with the coating agent (typically of a ~1.5 mm-thick layer). After that, the sample was placed in an appropriate incubator and left open to the air regulated at 30 °C and 20 % RH over a period of 1 week, which resulted in formation of an iridescent 4Cl-CPC–silica hybrid composite in the shape of a cylinder. In relation to the selection of the coating solvent, DPhDMS, MTMS, and DMDMS were also examined for the element instead of PhTMS, but eventually useless because of their worse gel formation inferior in the firmness or uniformity to PhTMS'.

The as-prepared 3Cl-CPC–silica and 4Cl-CPC–silica hybrids were taken out from the glass vials by breaking the walls with a hummer. The cylindrical bulk and disk-like flakes of each sample were grouped together and, usually, washed with distilled water and dried at 25–30 °C. The hybrid samples were kept in a desiccator until used for necessary measurements. As regards the 4Cl-CPC–silica series giving a larger surplus in amount, ca. 8 g of the samples was ground into granules (ϕ < ~150 μm) with an agate mortar or a ball mill, in order to use as adsorbent filler for column chromatography (see below).

2.5. Measurements

For structural characterization of CPC derivatives, ^{1}H NMR spectra were measured using a Varian NMR system 500 MHz with an oneNMR 5MM probe in the following conditions: solvent, dimethyl sulfoxide (DMSO)-d_6; temperature, 23 °C; solute concentration, 10 mg mL^{-1}; internal standard, tetramethylsilane (TMS); recycle time, 7.5 s; scan number, 128. Elemental analysis was made with a Yanaco CHN Corder MT series (for C, H, and N quantifications) and a combustion ion chromatography system XS-100 constituted of an ion chromatograph pretreatment unit AQF-100 (Mitsubishi Chemical Analytech, Co., Ltd.) and an ion chromatgraph ICS-1500 (Dionex Corp.) (for Cl quantification).

Polarized optical microscopy (POM) was conducted to verify the optical anisotropy of concentrated solutions by using an Olympus microscope BX60F5 equipped with a Mettler FP82HT/FP90 hot stage. The solutions (~10 mg) were sandwiched between a slide and cover glass and quickly sealed therein with plastic cement. Selective light-reflection of mesomorphic samples (solutions and hybrid composites) were examined by recording the reflection bands on an ultraviolet–visible–near-infrared (UV–Vis–NIR) spectrometer (Hitachi U-4100) equipped with a thermoregulated cell holder. Circular dichroism (CD) spectra were also measured for selected samples using a Jasco J-820DH spectropolarimeter equipped with

a Peltier-type temperature controller PTC-423L, to determine the handedness of the chiral nematic helical structure. These spectral measurements were conducted in an optical alignment of the normal incidence of light beam to the surface plane of each filmy or disk-like specimen. Refractive index measurements were carried out using an Abbé refractometer (Atago Co., Ltd., Type 2T) with a polarizer rotatable over the eyepiece. For mesomorphic solutions, the principal refractive indices parallel ($n_{\parallel}$) and perpendicular ($n_{\perp}$) to the plane of the prism surfaces were read off, and an average refractive index ($\tilde{n}$) was calculated by $\tilde{n} = (2n_{\parallel} + n_{\perp})/3$.

Wide-angle X-ray diffraction (WAXD) measurements were made using a Rigaku Ultima IV diffractometer in reflection mode, to examine the distance (d) and angular difference of rotation (φ) between adjacent thin nematic layers stacking in the mesophase of anisotropic samples. Nickel-filtered CuKα (0.1542 nm) radiation was utilized at 40 kV and 40 mA. Fluid samples were loaded into a copper holder 0.50 mm high and covered with a polyethylene (PE) wrapping film. The diffraction intensity profiles were collected in a range of 2θ = 2–40°.

To confirm the progress of sol–gel conversion of the alkoxysilane components (APTMS and TMOS), Raman spectra were measured using a Horiba LabRam-350V microscopic Raman spectrometer with an exciting laser of 632.85 nm. The measurements were made at ~20 °C via accumulation of 16 scans over a wavenumber range of 300–4000 cm^{-1} for hybrid composites and their parent solutions, and the obtained spectra of each pair were compared. For selected hybrids, which were as-cast ones with no further washing and drying, solid-state ^{29}Si MAS NMR measurements were performed in a Varian NMR system 400 MHz, to evaluate the progress of polycondensation of the alkoxysilane components. The apparatus was operated at a ^{29}Si frequency of 79.44 MHz, and the magic-angle spinning rate was 15.0 kHz. 1024 scans were accumulated to obtain a single-pulse ^{29}Si NMR spectrum, with a 90° pulse width of 4 μs and a recycle delay of 200 s. In the measurement, the sample was mixed with a proper quantity of powdered poly(dimethyl silane) (PDMS) as an internal standard (chemical shift, −34.44 ppm).

Column chromatography was conducted to separate a racemate of *trans*-stilbene oxide (TSO) into two enantiomers ((*R*,*R*)-TSO and (*S*,*S*)-TSO). The column was prepared in the following way: About 7 g of 4Cl-CPC–silica granules (sieved at $\phi \leq$ ~120 μm) was added to 10 mL of hexane/2-propanol (9:1, v/v), and the resulting slurry was poured into a glass tube (20 cm ht × 1.5 cm ϕ) in which cotton balls (~0.04 g per piece) and sand grains (~0.5 cm^3 per piece) were packed in advance. After the liquid flew out of the tube, additional sand grains

were loaded to press the substantial filler part (~14 cm ht). The column tube was saturated with a fresh 9:1 hexane/2-propanol mixture (~50 mL) for 24 h, until injection of the sample TSO (0.1 g dissolved in 1.5 mL of the same mixed solvent). Chromatograms were made in the following conditions: eluent, hexane/2-propanol (9:1); flow rate, ~0.3 mL min^{-1}; temperature, 23 °C; collection of effluent, total 80 fractions for a period of 160 min by collecting a ~0.5 mL volume per fraction; detection of TSO, UV absorbance at $\lambda_{max} \approx 273 \pm 2$ nm in the specific absorption band of 250–290 nm.

3. Results and discussion

3.1. Basic characterization of CPC derivatives

3.1.1. Molecular structure analysis

The CPC derivative samples synthesized in this study are listed in Table 1, together with values of the structural parameters, DS (degree of substitution), MS (molar substitution), and DP_s (degree of polymerization in the side chains); DS and MS denote the average number of substituted hydroxyls (≤ 3) and that of all phenylcarbamoyl entities introduced, respectively, per AGU of cellulose, and DP_s is defined as the average degree of phenylcarbamoyl polyaddition for the modified sites [29]. The evaluation of these parameters for 3Cl-CPC and 4Cl-CPC was made using ^{1}H NMR and elemental analysis data. To take an example, Fig. 3 illustrates a ^{1}H NMR spectrum obtained for a 4Cl-CPC sample (4Cl-$CPC_{2.69}$, Table 1) in DMSO-d_6. The assignment of resonance peaks is based on literature data for phenylcarbamate derivatives of chitinous polysaccharides [29,30]. A total area of the peaks derived from the amide protons of urethane and allophanate is designated as [A], and [B] refers to a peak area associated with the aromatic protons. Then, DP_s of the sample can be calculated by Eq. (1).

$$DP_s = ([B]/4) / [A] \quad (1)$$

The molar substitution MS is determinable by using the relative contents of C and Cl obtained from the elemental analysis. Generally, the carbons constituting a 4Cl-CPC (or 3Cl-CPC) product include 6 carbons in the AGU and 7×MS carbons of the chlorophenylcarbamoyl groups introduced per AGU, while the number of chlorine in the product is 1×MS per AGU. Therefore, the following equation holds:

$$([C]/12.01) / ([Cl]/35.45) = (6 + 7\times MS) / MS \quad (2)$$

where [C] and [Cl] are the weight fractions of C and Cl, respectively. The parameter DS is calculated by Eq. (3) according to the definition.

$$DS = MS / DP_s \quad (3)$$

As for the CPC reference ($CPC_{2.88}$, Table 1) containing no chlorine, the three parameters were determined by a method using two ^{1}H NMR data obtained separately with different solvents, DMSO-d_6 and CF_3COOD [29].

Table 1. Cellulose phenylcarbamate derivatives prepared in the present study

Sample code	In-feed isocyanate molar ratio (equiv AGU^{-1})	Reaction temperature (°C)	Reaction time (h)	DS	MS	DP_s
3Cl-$CPC_{2.41}$	7.5	25	72	2.41	2.55	1.06
3Cl-$CPC_{2.70}$	7.5	25	48	2.70	2.92	1.08
3Cl-$CPC_{2.99}$	10	60	120	2.99	3.20	1.07
4Cl-$CPC_{2.58}$	10	60	72	2.58	2.68	1.04
4Cl-$CPC_{2.60}$	10	60	72	2.60	2.80	1.08
4Cl-$CPC_{2.69}$	10	60	96	2.69	2.90	1.08
4Cl-$CPC_{2.76}$	10	60	96	2.76	2.84	1.03
4Cl-$CPC_{2.86}$	7.5	60	72	2.86	3.08	1.08
4Cl-$CPC_{2.90}$	10	60	96	2.90	3.01	1.04
$CPC_{2.88}$	7.5	50	96	2.88	3.09	1.07

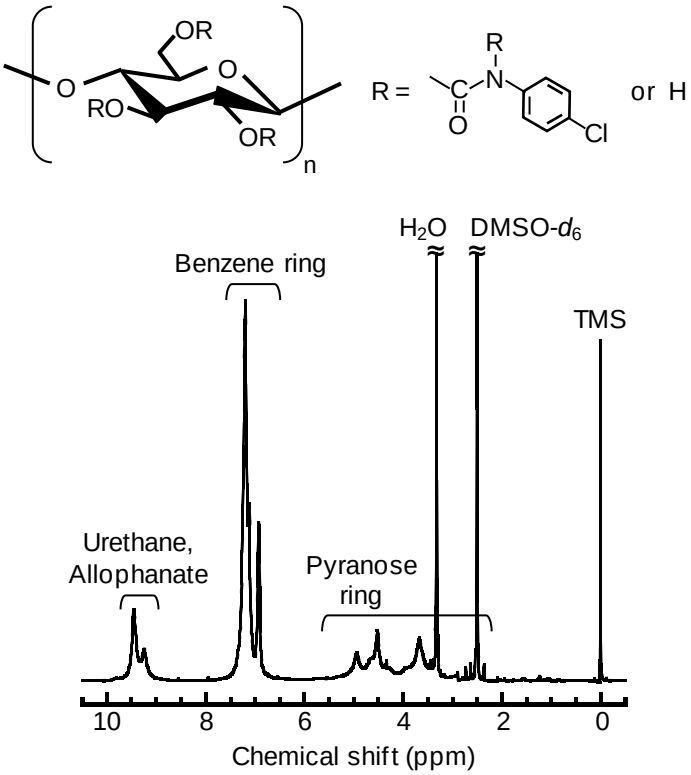

Fig. 3. ^{1}H NMR spectrum of a 4Cl-CPC sample (4Cl-$CPC_{2.69}$, Table 1) in DMSO-d_6.

As can be seen from Table 1, we successfully obtained mostly high-substituted CPC derivatives: 3Cl-CPCs of DS ≈ 2.4–3.0 and MS ≈ 2.6–3.2; 4Cl-CPCs of DS ≈ 2.6–2.9 and MS ≈ 2.7–3.1; CPC reference of DS ≈ 2.9 and MS ≈ 3.1. The high values of DS and MS can be attributed to the present conditions using fairly long reaction times and high concentrations of in-fed isocyanate [29]. Hereafter, a derivative sample, e.g., 3Cl-CPC of DS = *x* is encoded as 3Cl-CPC$_x$, if the specification is necessary.

3.1.2. Solubility and liquid crystallinity

The CPC derivatives listed in Table 1 were all less soluble in any of the assorted alkoxysilanes (see Sect. *2.1*) except APTMS, which was tested at a polymer concentration of 1–1.5 wt% at room temperature (~25 °C). In the employment of APTMS, the derivatives dissolved in this solvent even at 40 wt%, irrespective of the DS/MS values estimated above. The 40 wt% 3Cl-CPC/APTMS solutions were optically anisotropic and visually colored, as in the case using DMF for the solvent. Contrastively, the 40 wt% 4Cl-CPC and neat CPC solutions in APTMS were optically isotropic, differing from their mesophase formation at the same concentration in DMF. Table 2 instantiates the observations of the solubility and mesomorphy of representative samples at 40 wt%. At a higher concentration of 50 wt%, any derivative of the three sorts did not completely dissolve in APTMS, whereas, in DMF, the 3Cl-CPC and 4Cl-CPC samples still assumed the state of colored liquid-crystalline solution and the CPC reference formed an anisotropic gel of less fluidity.

Table 2. Mesophase formability of CPC derivatives in various solvents[a]

Polymer sample	Solvent			
	APTMS	DMF	TMOS/DMF[b]	TMOS/DMF/DCA (6:3:2)
3Cl-CPC$_{2.99}$	A (colored)	A (colored)	I	–
4Cl-CPC$_{2.90}$	I	A (colored)	A (colored)	A (colored)
CPC$_{2.88}$	I	A (colored)	×	–

[a] Examined at a polymer concentration of 40 wt% and at room temperature (~25 °C).
[b] 1:1 Mixture containing DCA at 1–2 wt%.
Notations: A, anisotropic (liquid-crystalline); I, isotropic; ×, incompletely dissolved; –, not prepared.

In order to attain the mesophase formation of 4Cl-CPC in solutions containing a reactive alkoxysilane, we next examined a mixture of TMOS and DMF for the availability as the suitable solvent (see Table 2). As a result, the 4Cl-CPC products dissolved well in a mixed solvent of TMOS/DMF = 1:1 (in wt) and the 40 wt% solutions each became a colored liquid

crystal. Another mixture of TMOS/DMF/DCA = 6:3:2 (in wt) was also found to be the relevant solvent to realize the liquid crystal of 4Cl-CPC. This solvent composition with higher contents of TMOS and DCA would be more practical for the purpose of the present study. The acid component DCA, which showed an adequate dissolvability to the CPC derivatives, can serve to catalyze the sol–gel process of TMOS. Incidentally, however, it is unrealistic to use DCA together with the basic alkoxysilane, APTMS.

3.2. Chiral nematic properties of 3Cl-CPC and 4Cl-CPC lyotropics

3.2.1. 3Cl-CPC/APTMS system

Solutions of the 3Cl-CPC products prepared at 36–40 wt% in APTMS were completely anisotropic and assumed a chiral nematic liquid-crystalline state. At concentrations of 32 and 34 wt%, the 3Cl-CPC solutions were biphasic and contained an optically isotropic phase dappled with liquid-crystalline domains. Fig. 4a illustrates selective light-reflection spectra measured for the 36, 38, and 40 wt% 3Cl-CPC$_{2.99}$/APTMS solutions (20 °C) together with color photographs of their visual appearance. The photographs were obtained through digital scanning of the bottom of each individual sample vial at room temperature (~20 °C). It is found that the wavelength λ_M giving the reflectance maximum shifts to the blue side with increasing polymer concentration, indicating the negative dependence of the chiral nematic pitch (P) on the concentration. In CD measurements, the 3Cl-CPC$_{2.99}$/APTMS lyotropics exhibited CD spectra characterized by a negative ellipticity curve in the selective light reflection, as shown in Fig. 4b. This indicates development of a "right-handed" chiral nematic structure in each solution.

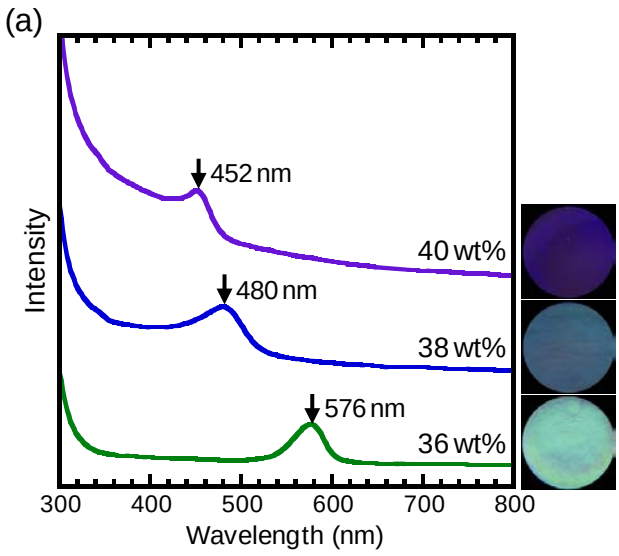

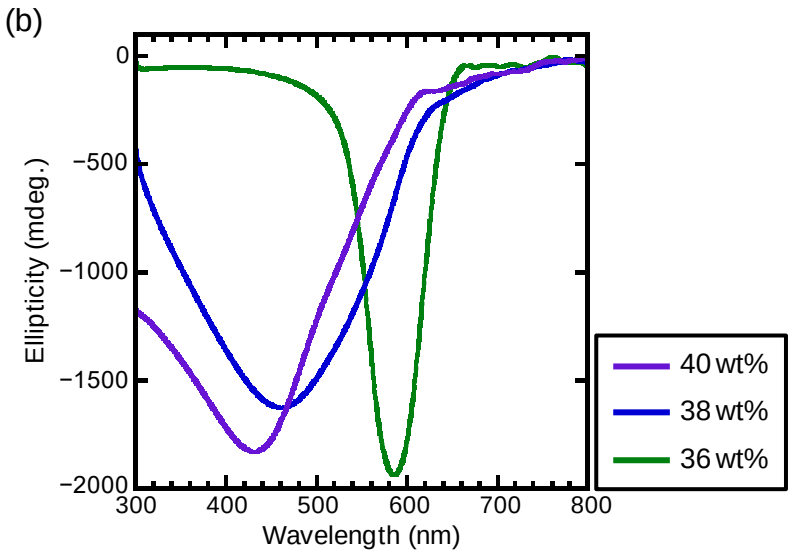

Fig. 4. Optical characterization for 3Cl-CPC lyotropics (right-handed chiral nematics) in APTMS: (a) selective light-reflection spectra of 36, 38, and 40 wt% 3Cl-CPC$_{2.99}$/APTMS solutions (20 °C) detected by a UV–Vis–NIR photometer, and photographs of visual appearance of the corresponding samples; (b) CD spectra of the same solutions as those used in (a).

Concerning DS dependence of the pitch *P* in the 3Cl-CPC/APTMS lyotropics, this value and therefore λ_M tended to shift to shorter wavelengths with increasing DS in the explored range of 2.41–2.99, suggesting a negative correlation between *P* and DS (namely, the increase in 3-chlorophenylcarbamoyl DS seems to strengthen the right-handed twisting power). With regard to temperature dependence of the pitch, the selective light-reflection measurements revealed a systematic shift of λ_M to shorter wavelengths with elevating temperature, i.e., a negative correlation between *P* and temperature, in the limits below an isotropization temperature (T_i). This phase transition temperature was estimated by POM observation (see Supplementary Information, Fig. S1), for example, as T_i = ~70 °C for 3Cl-CPC$_{2.99}$/APTMS and ~50 °C for 3Cl-CPC$_{2.41}$/APTMS at a 3Cl-CPC concentration of 36 wt%. The right-handed chiral nematic arrangement was always retained irrespective of variations in the DS and temperature, as far as the lyotropics were placed at temperatures below the individual T_i.

3.2.2. 4Cl-CPC/TMOS/DMF/DCA system

Solutions of the 4Cl-CPC products (DS ≈ 2.6–2.9, Table 1) were prepared at 32–48 wt% in the mixed solvent, TMOS/DMF/DCA (6:3:2 in wt). The solutions were mostly isotropic at the polymer concentrations of ≤36 wt%, whereas, at 40 wt% and higher concentrations,

they were totally anisotropic and formed a clear chiral nematic mesophase. Fig. 5a exemplifies selective light reflection spectra and visual appearance data for 40, 44, and 48 wt% 4Cl-CPC$_{2.69}$ solutions in TMOS/DMF/DCA (20 °C). It is observed that the λ_M position shifted to lower wavelengths as the 4Cl-CPC concentration increased, indicating an ordinary negative dependence of the pitch P on the concentration. From CD data (Fig. 5b), the rotational sense of the chiral nematic helical structure in the lyotropics was found to be "left-handed," because the spectra gave a positive ellipticity signal in the wavelength range of the selective light reflection; this situation is the exact opposite to the case in the 3Cl-CPC lyotropic series.

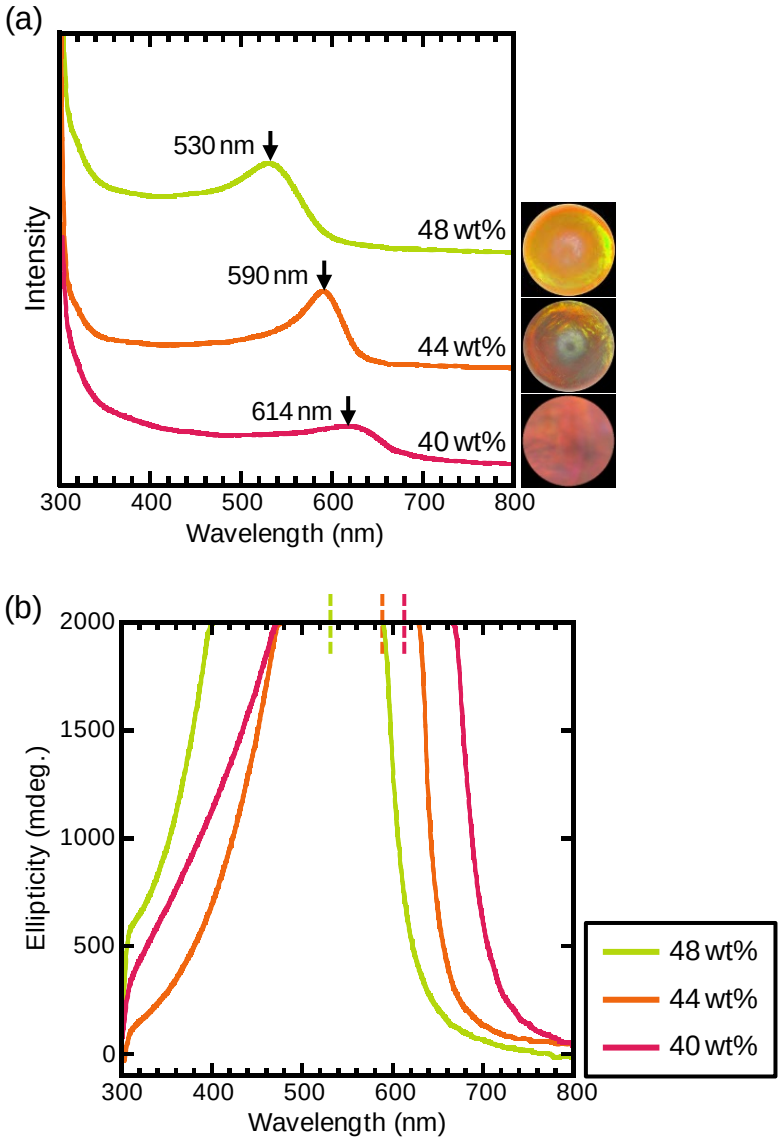

Fig. 5. Optical characterization for 4Cl-CPC lyotropics (left-handed chiral nematics) in TMOS/DMF/DCA (6:3:2 in weight ratio): (a) selective light-reflection spectra and visual appearance data for 40, 44, and 48 wt% 4Cl-CPC$_{2.69}$/TMOS/DMF/DCA solutions (20 °C); (b) CD spectra of the same samples as those used in (a). The observed CD signals were so large

that the peak tops were out of the measurable range. Vertical broken-lines represent a λ_M position determined by UV–Vis–NIR spectrophotometry.

In comparative measurements using various 4Cl-CPC samples of DS = 2.60–2.90, the spectral λ_M observed for the lyotropics slightly shifted to the blue side with increasing DS, but the reflective colors to the naked eye were almost indistinguishable from each other (e.g., the 45 wt% solutions were all reddish). Thus the increase in 4-chlorophenylcarbamoyl DS in the explored range did not noticeably reinforce the left-handed twisting power. In similar spectral measurements at different temperatures ranging from −10 to 30 °C, the 4Cl-CPC lyotropic series showed a positive dependence of λ_M (and P) on the varying temperature (e.g., λ_M = 554 nm at 0 °C and λ_M = 654 nm at 30 °C in the use of 4Cl-CPC$_{2.90}$ at 45 wt%). This is in contrast to the P vs. temperature behavior of negative correlation found for the 3Cl-CPC lyotropic series. The anisotropic to isotropic phase transition of the 4Cl-CPC lyotropics occurred commonly at a temperature intermediate between 40 and 50 °C; i.e., roughly $T_i \approx$ 45 °C (see Fig. S1b). However, it was confirmed by CD polarimetry that the supramolecular helical structure in the 4Cl-CPC chiral nematics remained left-handed at least below 40 °C.

3.3. Mesomorphic structure and properties of 3Cl-CPC–silica and 4Cl-CPC–silica hybrids

3.3.1. Characterization of the fixed chiral nematic order

3Cl-CPC–silica hybrids were prepared in a cylindrical form from the 3Cl-CPC/APTMS lyotropics by sol–gel conversion of APTMS in an open system. In this method, moisture absorbed by each lyotropic sample is involved in the hydrolysis reaction and methanol/water (by-products) can be vaporized to advance the polycondensation reaction (see Scheme 1). In the actual casting process, the solidification of the parent solution in a vial proceeded from the surface toward the bottom layer, which was ultimately followed by ~10 % reduction in volume of the sample. It seemed that the solvent APTMS partly evaporated without wholly reacting in the gelation process. Concomitantly, the reflective coloration of the sample turned into the one of shorter wavelengths after the gelation; for instance, a color change from light blue into pale violet was observed in the processing of a 38 wt% 3Cl-CPC$_{2.99}$/APTMS solution. Fig. 6 illustrates CD spectra of 3Cl-CPC$_{2.99}$–silica hybrids prepared from 36, 38, and 40 wt% 3Cl-CPC$_{2.99}$ solutions in APTMS by the sol–gel method. The data shows that the hybrids reflect right-handed circularly polarized lights as did the original concentrated solutions, although the reflection peak (λ_M) is situated at a shorter wavelength relative to that observed for the respective parent samples (see Fig. 4b).

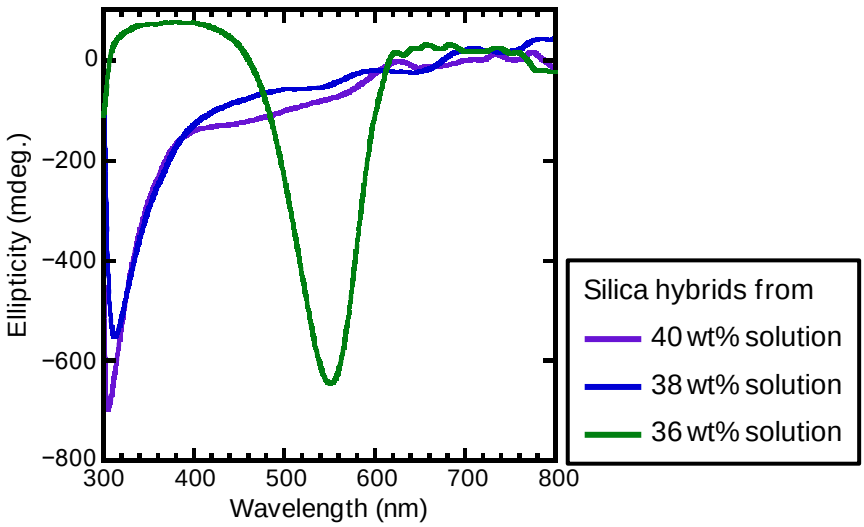

Fig. 6. CD spectral data for 3Cl-CPC$_{2.99}$–silica hybrids prepared from 36, 38, and 40 wt% solutions of 3Cl-CPC$_{2.99}$ in APTMS by the sol–gel conversion method.

As regards the fixation of mesomorphic structure for the 4Cl-CPC lyotropic series by the sol–gel phase inversion, we invented a coating technique with a TMOS/PhTMS/DCA (1:1:1) mixture; specifically, the surface of each liquid-crystalline 4Cl-CPC solution in TMOS/DMF/DCA (6:3:2) was covered with the coating solvent and the system whole was thermostated at 30 °C and 20 % RH in an incubator for 1 week. Thereby, 4Cl-CPC–silica hybrids were obtained as a monolithic glassy bulk that imparted iridescent colors, which indicates that the chiral nematic structure was successfully immobilized in the silica gel matrix. No appreciable shrinkage in volume of the samples was perceived after the conversion from their fluid state, but yet the iridescence of each hybrid shifted to colors of shorter wavelengths when compared with the parent solution. Fig. 7a illustrates selective reflection spectra of the hybrid samples prepared from 40, 44, and 48 wt% solutions of 4Cl-CPC$_{2.69}$ in TMOS/DMF/DCA, together with photographs of their visual appearance. By comparison with the optical data given in Fig. 5a, it can readily be seen that the reflection wavelengths (λ_M positions) of the hybrids moved to the blue side from the corresponding ones of the original liquid-crystalline solutions. From CD spectral data (Fig. 7b) providing a positive ellipticity signal, it is confirmed that the left-handed helical arrangement was preserved in the 4Cl-CPC–silica hybrids.

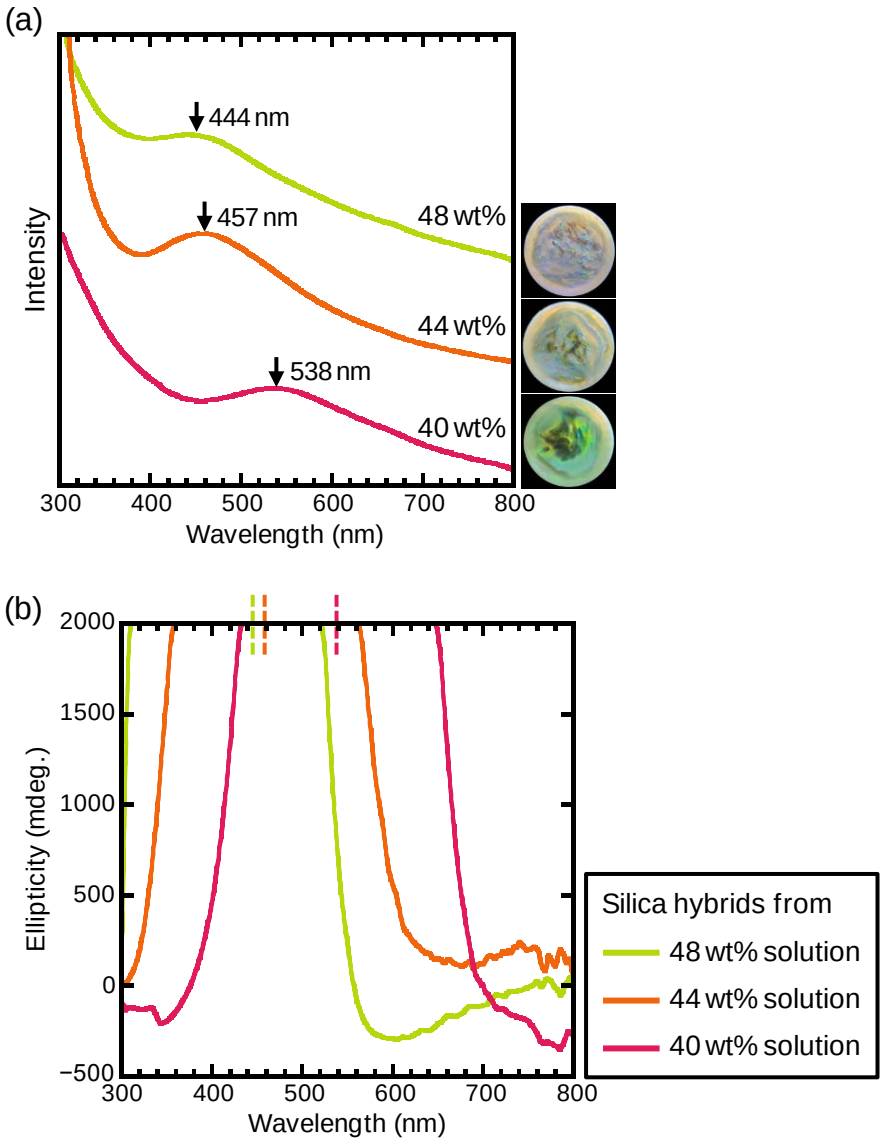

Fig. 7. Optical characterization for 4Cl-CPC–silica hybrids prepared from 40, 44, and 48 wt% solutions of 4Cl-CPC$_{2.69}$ in TMOS/DMF/DCA (6:3:2) by the sol–gel conversion method using a coating agent of TMOS/PhTMS/DCA (1:1:1): (a) selective light-reflection spectra and visual appearance data; (b) CD spectra. The CD signals were so large that the peak tops were out of the measurable range. Vertical broken-lines represent a λ_M position determined by UV–Vis–NIR spectrophotometry.

In the sol–gel processing for the 4Cl-CPC lyotropics, the reaction started in the upper coating solvent and then proceeded to the lower concentrated solution. A relatively tight network of silica gel would be formed in the outer coat, which should contribute to minimize the amount of water absorbed inward from the atmosphere. Instead of the external moisture, the water produced in the condensation reaction of TMOS/PhTMS would be utilized for the following hydrolysis in the contiguous lower part. The methanol as a by-product of the hydrolysis would be allowed to diffuse into the upper coating side so as to promote the next

reaction cycle, while non- or partially hydrolyzed alkoxysilanes would penetrate the further lower solution phase. Additionally, PhTMS having a phenyl and three methoxyl groups could serve as a moderate diluent (i.e., compatibilizer) for the mutually repellent 4Cl-CPC and TMOS components. Under these favorable conditions, the continuous sol–gel conversion would successfully proceed in the semi-closed lyotropic system, without inviting phase-separation of 4Cl-CPC from the hygroscopic TMOS-rich solvent. Here it should be remarked that the hybrid samples subjected to various measurements were prepared via the total process including the finishing treatment of rinse and drying in addition to the sol–gel reaction. In view of the full elimination of diffusible minor components (methanol/water and DMF/DCA) from the gel system, the hybrids would be endowed with a microporous organization as a kind of xerogel.

Next we make a quantitative comparison of the helical or twisting power of chiral nematic layered structure between the 4Cl-CPC lyotropics (Fig. 5) and corresponding hybrids with silica (Fig. 7). The power may be characterized in terms of a set of two parameters, the normal distance d and azimuth difference φ between adjacent nematic thin layers, as depicted in Fig. 1. For the insight into the short-range order, the chiral nematic pitch P was quantified in advance by using the de Vries equation [32], $P = \lambda_M / \tilde{n}$, where $\tilde{n}$ is an average refractive index of the mesomorphic medium. Table 3 lists P values determined for the 40, 44, and 48 wt% 4Cl-CPC$_{2.69}$ lyotropics. In this calculation, the following optical data were used: $\lambda_M / \tilde{n}$ = 614 nm /1.484 (for 40 wt%); 590 nm /1.493 (for 44 wt%); 530 nm /1.502 (for 48 wt%). Concerning the 4Cl-CPC$_{2.69}$–silica hybrids (disk-like specimens), their refractive indices were not well measurable due to the surface roughness; hence, the values were approximated as $\tilde{n}$ = 1.48–1.53 which covers the index values (ca.1.49–1.52) of standard silica glasses as well as those of the parent lyotropic samples. Using the λ_M data of 538, 457, and 444 nm observed for the hybrids (see Fig. 7a), we made a rough estimate of the P values, as summarized in Table 3.

Table 3. Values of the helical pitch (P), interlayer distance (d), twist angle (φ), and twisting power (φ/d) in the chiral nematic layered structure, estimated for 4Cl-CPC$_{2.69}$ lyotropic solutions (20 °C) and 4Cl-CPC$_{2.69}$–silica hybrids

4Cl-CPC conc. (in feed) (wt%)	4Cl-CPC lyotropic				4Cl-CPC–silica hybrid			
	P (nm)	d (nm)	φ (deg)	φ/d (deg·nm^{-1})	P (nm)	d (nm)	φ (deg)	φ/d (deg·nm^{-1})
40	414	1.52	1.32	0.868	358 ± 6	1.66	1.67 ± 0.03	1.01 ± 0.02
44	395	1.52	1.39	0.914	304 ± 5	1.65	1.95 ± 0.03	1.18 ± 0.02

48	353	1.51	1.54	1.02	295 ± 5	1.64	2.00 ± 0.03	1.22 ± 0.02

Fig. 8 collects WAXD intensity curves acquired for the 4Cl-CPC$_{2.69}$–silica hybrids and corresponding original 4Cl-CPC$_{2.69}$ solutions. All the diffraction data gave only one significant peak at a lower angular position of 2θ = 5.3–5.4° (for hybrids) or 5.8–5.9° (for lyotropics), except for a diffuse scattering halo centered at $2\theta \approx 20°$. The low-angle diffraction reflects a short-range order of mesogenic 4Cl-CPC chains arranged in a quasi-hexagonal manner [29,31]; the observation of a rather broader peak for the solutions may be ascribed to the greater fluctuation of the polymer molecules therein. Assuming the hexagonal approximation, the distance d between the nematic layers constructing the mesophase can be directly estimated from the low-angle data by Bragg's equation ($2d \sin\theta = \lambda$, λ = 0.1542 nm). Then, the twist angle φ, defined as the angular difference in orientation between adjacent nematic layers, is calculable from the relation $\varphi = 360° \times d/P$. Table 3 includes the result of the d and φ quantifications for the mesomorphic samples concerned. The interlayer distance d slightly increased from 1.51–1.52 to 1.64–1.66 nm in consequence of the sol–gel conversion of the 4Cl-CPC lyotropics, although the chiral nematic pitch P decreased seriously then. Instead, the angle φ increased so as to strengthen the twisting power (φ/d) of the chiral nematic arrangement, resulting in the marked diminution of P. Presumably, the chemical reaction of TMOS (yielding a siloxane linkage) in the lyotropic solvent would alter the chiral interlayer interaction associated with a certain chiral conformation (helical or twisted form) of the constituent 4Cl-CPC chains. This must cause the change in the twist angle φ.

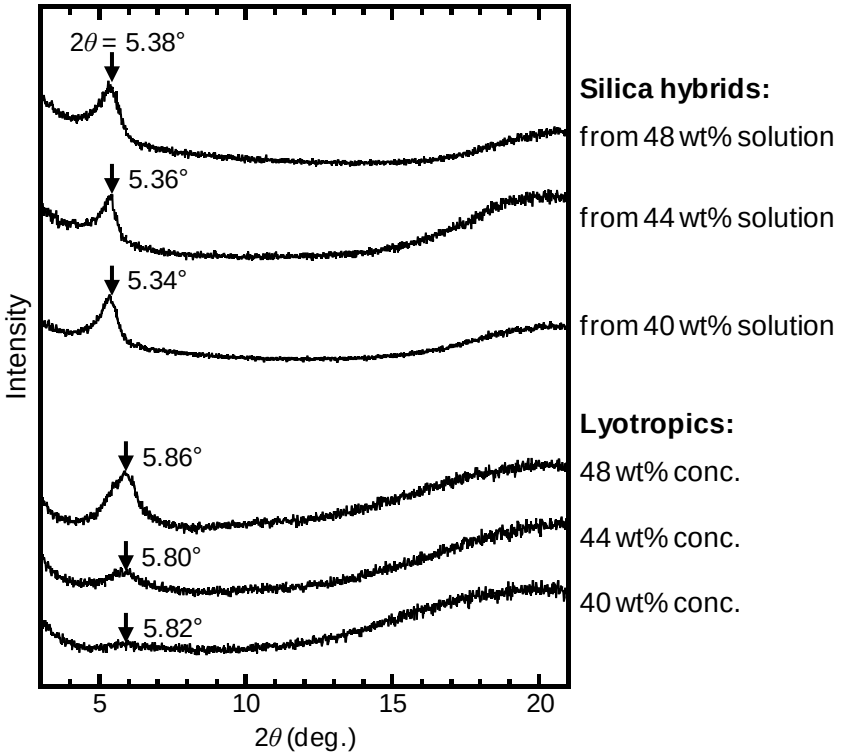

Fig. 8. WAXD intensity profiles obtained for 4Cl-CPC$_{2.69}$–silica hybrids (upper three) and parent 4Cl-CPC$_{2.69}$ lyotropics (lower three) of 40, 44, and 48 wt% polymer in feed. Arrows indicate a peak position for the low-angle diffraction.

3.3.2. Evaluation of the sol–gel conversion by Raman and ^{29}Si NMR spectroscopy

Raman spectra obtained for a 4Cl-CPC$_{2.69}$ lyotropic sample (48 wt% polymer conc.) and its gelled hybrid are shown in Fig. 9a; the assignment of major peaks is based on literature data [33,34]. Comparing the two spectral data, we readily find a few significant changes in chemical structure given rise to by the sol–gel conversion: (1) A C–H stretching peak (~2840 cm^{-1}) associated with the methoxyl group of TMOS [33], observed for the concentrated solution, completely disappears in the hybrid (rinsed and dried). (2) A Si–OH stretching peak (~980 cm^{-1}) appears in the hybrid only. These findings evidence a good progress of the hydrolysis reaction of the TMOS component. (3) A Si–O symmetric stretching signal (~650 cm^{-1}) of TMOS is seriously suppressed by the sol–gel conversion. This suppression can support the progress of the hydrolysis and successive condensation of the alkoxysilane component [34]. Similar observations relating to the reaction of Si alkoxides were made in a comparative Raman study for the 3Cl-CPC series of lyotropics and hybrids.

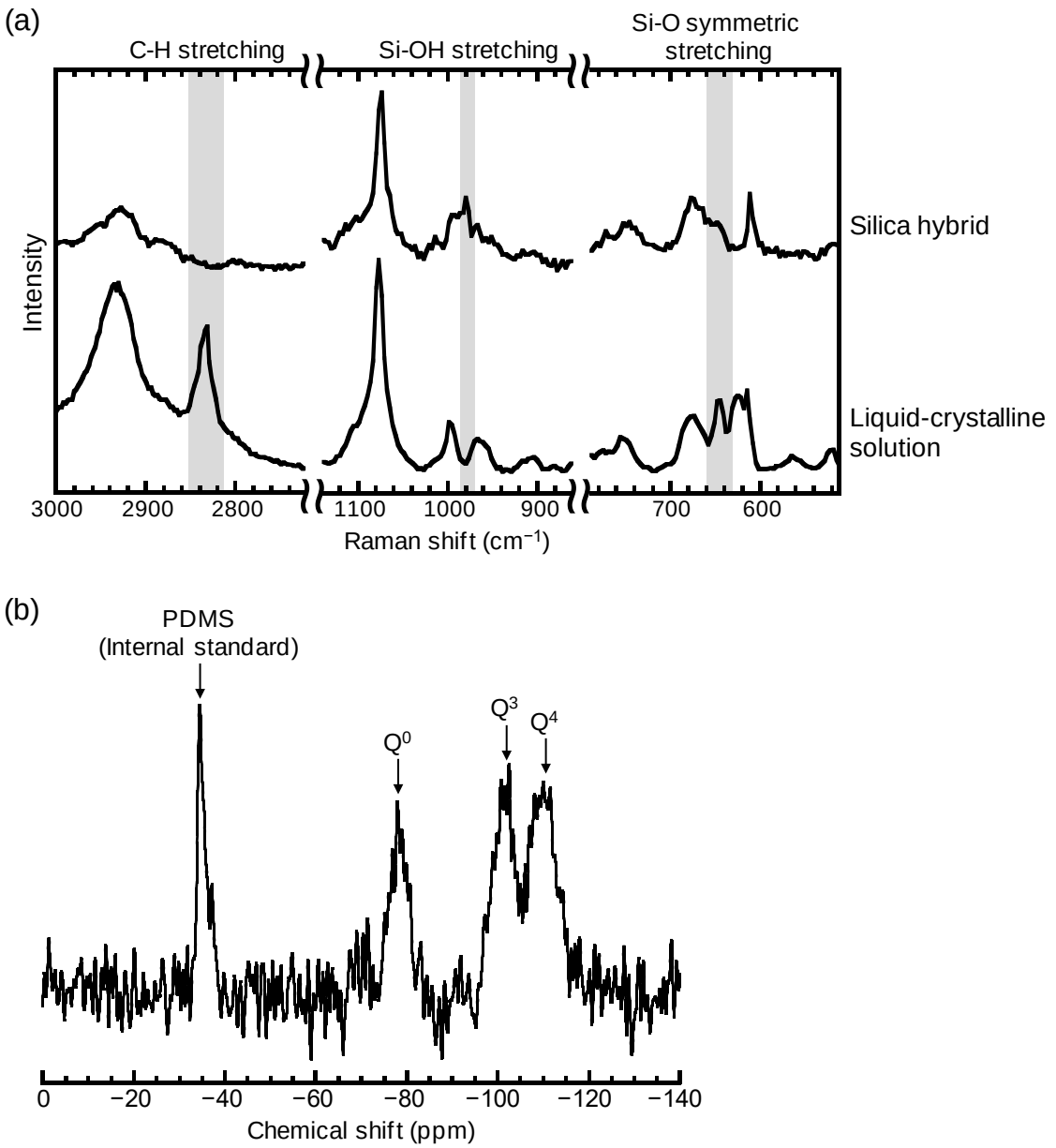

Fig. 9. (a) Raman spectra for a set of samples, 4Cl-CPC$_{2.69}$ solution (48 wt%) in TMOS/DMF/DCA and 4Cl-CPC$_{2.69}$–silica hybrid (fully dried), the two data being compared in three separate regions of frequency. (b) Solid-state ^{29}Si MAS NMR spectrum of a 4Cl-CPC$_{2.69}$–silica hybrid (~45 wt% 4Cl-CPC), this sample being used without washing treatment.

Fig. 9b shows a ^{29}Si MAS NMR spectrum obtained for a fresh hybrid of 4Cl-CPC$_{2.69}$–silica (~45 wt% 4Cl-CPC); the sample was used without treatment of rinse and drying. The ^{29}Si NMR data provides information on the overall extent of reaction (esp., polycondensation) of TMOS and even identifies the types of Si-linking structures (i.e., Q^n species) developed in the silica-hybridized material. The specific symbol represents Q^n = Si(OSi)$_n$(OH)$_{4-n}$, with n (= 0–4) that is the number of bridging oxygens for siloxane. In the

presented data, we can see three explicit resonance peaks except a reference peak (−34.44 ppm) derived from PDMS as internal standard. The two large peaks situating at ca. −110 and −102 ppm can be assigned to Q^4 [$(SiO)_4$–Si] and Q^3 [$(SiO)_3$–SiOH] structures, respectively [35]. This observation indicates a well development of siloxane bonds and confirms the progress of polycondensation of TMOS. Meanwhile, however, the NMR data imparts another peak appearing at −78 ppm; this resonance signal can be assigned to Q^0 [$Si(OH)_4$] [36]. It is therefore suggested that some amount of TMOS remained uncondensed after the hydrolysis into silanols, without taking part in the network formation of Si–O–Si bonds. It may be supposed that the polycondensation proceeded in a very slow kinetics, probably due to the limited evaporation of water from the equilibrium reaction system. Additionally remarking, the two species, Q^2 [$(SiO)_2$–$Si(OH)_2$] (ca. −92 ppm) and Q^1 [(SiO)–$Si(OH)_3$] (ca. −84 ppm) [36], were almost indiscernible in the NMR data.

3.3.3. Preliminary examination of the chiral separation of enantiomers

Finally, we attempted to separate a racemate of *trans*-stilbene oxide, TSO, into two enantiomers ((*R*,*R*)-TSO and (*S*,*S*)-TSO) by open column chromatography using mesomorphic 4Cl-CPC–silica hybrids as the column filler. Fig. 10 illustrates a data of the chromatogram detected by UV absorption. The data exhibits a very broad peak over a range from 40 to 120 min of elution time. The peak seems to be somewhat bimodal and composed of two signals, one centering at 60 min and the other around 90 min, as guided by dotted-line curves in the figure. Virtually, however, we cannot find clearly discrete separation of the enantiomers in the chromatogram. It is known that 4Cl-CPC has an ability of chiral recognition to TSO and other racemic compounds, and silica gels (in particle form) on which the cellulosic derivative is coated can serve as a chiral stationary phase for HPLC [37]; usually, an isotropic solution of the polymer is used for the coating. The present observation of an imperfect enantioseparation may be ascribed principally to inefficient contacts of the hybrid fillers with the solute, originating from their relatively large sizes (>100 μm) of non-uniformity. For further investigation into the chiral resolution, the sizes of the hybrid fillers should be regulated to have uniformity in the order of ≤10 μm [25,27]; thereby the evaluation in HPLC conditions will also be feasible.

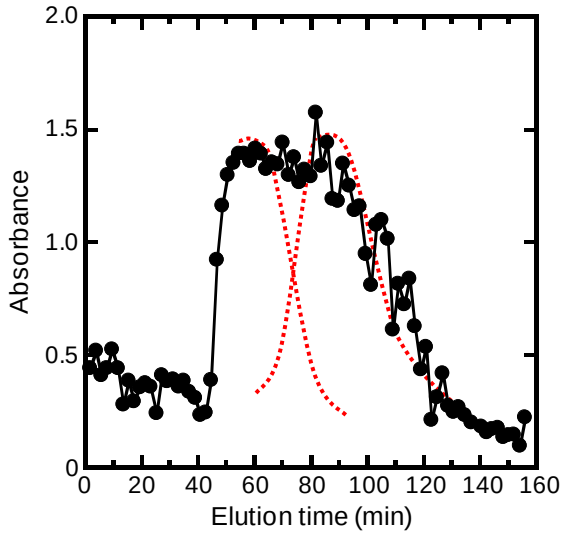

Fig. 10. Chromatogram data for a racemate of *trans*-stilbene oxide (TSO), obtained by open column chromatography using 4Cl-CPC–silica hybrid as the column filler. Conditions: eluent, hexane/2-propanol (9:1, v/v); flow rate, ~0.3 mL min^{-1}; temperature, 23 °C; UV detection wavelength, λ_{max} (273 ± 2 nm) at which the maximal absorbance was observed.

4. Conclusions

We synthesized highly substituted 3Cl-CPC and 4Cl-CPC in order to obtain liquid crystals using alkoxysilane for the solvent component and to attain novel mesomorphic composites with silica by sol–gel conversion of the lyotropic systems. Concentrated solutions of 3Cl-CPC (≥36 wt%) in APTMS formed a chiral nematic mesophase and visually imparted colors coming from selective light reflection. The handedness of the supramolecular helical arrangement was right-handed. The other derivative 4Cl-CPC also provided a colored, chiral nematic liquid crystal in a mixed solvent of TMOS/DMF/DCA at polymer concentrations of ≥40 wt%, but the helical sense in this chiral mesomorphy was left-handed.

The chiral nematic structures of the 3Cl-CPC and 4Cl-CPC lyotropics were successfully carried over into the corresponding hybrid composites, 3Cl-CPC–silica and 4Cl-CPC–silica, with retention of the initial handedness of helical arrangement. Both hybrid series showed iridescence, although the coloration shifted to the blue side of optical spectrum when compared to that of the parent lyotropics. In the process for preparing the 4Cl-CPC–silica series, we adopted a coating agent to control the amount of water involved in the hydrolysis/polycondensation of the alkoxysilane component. It was confirmed that the sol–gel reaction of the employed alkoxysilanes definitely progressed to yield siloxane links. Thus we demonstrated the first example of silica hybridization for hydrophobic derivatives of

cellulose in the liquid crystalline state.

In connection with the chiral recognition ability of CPC derivatives to enantiomers, we also attempted to separate a racemic compound (TSO) into two enantiomers by open column chromatography using the mesomorphic 4Cl-CPC–silica hybrids for the filler material. In the present experiment, the granular sizes of the prepared fillers were relatively larger and lack of uniformity, and we solely observed a chromatogram indicating incomplete resolution. With improved conditions in the filler size and column tube (to be adaptable for HPLC), the chiral resolution property of such cellulosic–silica hybrids will be examined in detail in the near future. Then it should be interesting to provide insight into a correlation between the chiral resolvability and the chiral nematic helical structure of the cellulosic derivatives.

Acknowledgments

This work was partially financed by Grant-in-Aids (KAKENHI) for Scientific Research (A) (No. 26252025 to YN) and Young Scientist Research (B) (No. 17K15295 to KS) from the Japan Society for the Promotion of Science (JSPS).

Appendix A. Supplementary data

Supplementary data related to this article can be found at https://doi.org/10.1016/j.polymer.2019.??.???.

References

[1] J.-X. Guo, D.G. Gray, Lyotropic cellulosic liquid crystals, in: R.D. Gilbert (Ed.), Cellulosic polymers, blends and composites, Hanser, Munich, 1994, Chapter 2.

[2] D.G. Gray, Chiral nematic ordering of polysaccharides, Carbohydr. Polym. 25 (1994) 277–284.

[3] P. Zugenmaier, Polymer solvent interaction in lyotropic liquid crystalline cellulose derivative systems, in: R.D. Gilbert (Ed.), Cellulosic polymers, blends and composites, Hanser, Munich, 1994, Chapter 4.

[4] P. Zugenmaier, Cellulosic liquid crystals, in: D. Demus, J. Goodby, G.W. Gray, H.-W. Spiess, V. Vill (Eds.), Handbook of liquid crystals, Wiley-VCH, Weinheim, 1998, Vol. 3 Chapter IX.

[5] Y. Habibi, L.A. Lucia, O.J. Rojas, Cellulose nanocrystals: chemistry, self-assembly, and applications, Chem. Rev. 110 (2010) 3479–3500.

[6] J. Araki, Electrostatic or steric? – preparations and characterizations of well-dispersed systems containing rod-like nanowhiskers of crystalline polysaccharides, Soft Matter 9 (2013) 4125–4141.

[7] Y. Nishio, J. Sato, K. Sugimura, Liquid crystals of cellulosics: fascinating ordered structures for the design of functional material systems, Adv. Polym. Sci. 271 (2016) 241–286.

[8] Y. Nishio, T. Yamane, T. Takahashi, Morphological studies of liquid-crystalline cellulose derivatives. I. Liquid-crystalline characteristics of hydroxypropyl cellulose in 2-hydroxyethyl methacrylate solutions and in polymer composites prepared by bulk polymerization, J. Polym. Sci., Polym. Phys. Ed. 23 (1985) 1043–1052.

[9] Y. Nishio, S. Susuki, T. Takahashi, Structural investigations of liquid-crystalline ethylcellulose, Polym. J. 17 (1985) 753–760.

[10] Y. Nishio, Material functionalization of cellulose and related polysaccharides via diverse microcompositions, Adv. Polym. Sci. 205 (2006) 97–151.

[11] T. Ogiwara, A. Katsumura, K. Sugimura, Y. Teramoto, Y. Nishio, Calcium phosphate mineralization in cellulose derivative/poly(acrylic acid) composites having a chiral nematic mesomorphic structure, Biomacromolecules 16 (2015) 3959–3969.

[12] A. Katsumura, K. Sugimura, Y. Nishio, Calcium carbonate mineralization in chiral mesomorphic order-retaining ethyl cellulose/poly(acrylic acid) composite films, Polymer 139 (2018) 26–35.

[13] K.E. Shopsowitz, H. Qi, W.Y. Hamad, M.J. MacLachlan, Free-standing mesoporous silica films with tunable chiral nematic structures, Nature 468 (2010) 422–425.

[14] M. Giese, L.K. Blusch, M.K. Khan, M.J. MacLachlan, Functional materials from cellulose-derived liquid-crystal templates, Angew. Chem. Int. Ed. 54 (2015) 2888–2910.

[15] E. Dujardin, M. Blaseby, S. Mann, Synthesis of mesoporous silica by sol–gel mineralisation of cellulose nanorod nematic suspensions, J. Mater. Chem. 13 (2003) 696–699.

[16] H. Dislich, Sol-Gel 1984 → 2004 (?), J. Non-Cryst. Solids 73 (1985) 599–612.

[17] S. Sakka, Science of Sol-Gel Processing (in Japanese), Agne-Shofu Pub., Tokyo, 1988.

[18] S. Sakka, Current sol-gel activities in Japan, J. Sol-Gel Sci. & Techn. 37 (2006) 135–140.

[19] A. Thomas, M. Antonietti, Silica nanocasting of simple cellulose derivatives: towards chiral pore systems with long-range order and chiral optical coatings, Adv. Funct. Mater. 13 (2003) 763–766.

[20] M.K. Khan, A. Bsoul, K. Walus, W.Y. Hamad, M.J. MacLachlan, Photonic Patterns Printed in Chiral Nematic Mesoporous Resins, Angew. Chem. Int. Ed. 54 (2015) 4304–4308.

[21] W.Y. Hamad, Photonic and semiconductor materials based on cellulose nanocrystals, Adv. Polym. Sci. 271 (2016) 287–328.

[22] J.-F. Revol, L. Godbout, D.G. Gray, Solid self-assembled films of cellulose with chiral nematic order and optically variable properties, J. Pulp Paper Sci. 24 (1998) 146–149.

[23] J. Majoinen, E. Kontturi, O. Ikkala, D.G. Gray, SEM imaging of chiral nematic films cast from cellulose nanocrystal suspensions, Cellulose 19 (2012) 1599–1605.

[24] P. Zugenmaier, Supramolecular structure of polysaccharides, in: S. Dumitriu (Ed.), Polysaccharides: structural diversity and functional versatility, Marcel Dekker, New York, 1998, Chapter 2.

[25] T. Ikai, Y. Okamoto, Structure Control of Polysaccharide Derivatives for Efficient Separation of Enantiomers by Chromatography, Chem. Rev. 109 (2009) 6077–6101.

[26] C. Yamamoto, Y. Okamoto, Optically Active Polymers for Chiral Separation, Bull. Chem. Soc. Jpn. 77 (2004) 227–257.

[27] T. Shibata, Polysaccharide as chiral stationary phase (in Japanese), Kobunshi (Journal of the Society of Polymer Science, Japan) 59 (2010) 416–417.

[28] D. Aoki, Y. Nishio, Phosphorylated cellulose propionate derivatives as thermoplastic flame resistant/retardant materials: influence of regioselective phosphorylation on their thermal degradation behaviour, Cellulose 17 (2010) 963–976.

[29] Y. Kuse, D. Asahina, Y. Nishio, Molecular structure and liquid-crystalline characteristics of chitosan phenylcarbamate, Biomacromolecules 10 (2009) 166–173.

[30] T. Matsubara, Y. Miyashita, Y. Nishio, Synthesis and structural characterization of phenylcarbamate derivatives of chitin and chitosan, Kobunshi Ronbunshu 67 (2010) 135–142.

[31] J. Sato, N. Morioka, Y. Teramoto, Y. Nishio, Chiroptical properties of cholesteric liquid crystals of chitosan phenylcarbamate in ionic liquids, Polym. J. 46 (2014) 559–567.

[32] H. de Vries, Rotatory power and other optical properties of certain liquid crystals, Acta Crystallogr. 4 (1951) 219–226.

[33] A. Bertoluzza, C. Fagnano, M.A. Morelli, V. Gottardi, M. Guglielmi, Raman and infrared spectra on silica gel evolving toward glass, J. Non-Cryst. Solids 48 (1982) 117–128.

[34] M.C. Matos, L.M. Ilharco, R.M. Almeida, The evolution of TEOS to silica gel and glass by vibrational spectroscopy, J. Non-Cryst. Solids 147 & 148 (1992) 232–237.

[35] P. Paik, A. Gedanken, Y. Mastai, Chiral separation abilities: Aspartic acid block copolymer-imprinted mesoporous silica, Micropor. Mesopor. Mater. 129 (2010) 82–89.

[36] J.J. van Beek, D. Seykens, J.B.H. Jansen, R.D. Schuiling, Incipient polymerization of SiO_2 in acid-catalyzed TMOS sol-gel systems with molar water/alkoxide ratio between 0.5 and 32, J. Non-Cryst. Solids 134 (1991) 14–22.

[37] Y. Okamoto, M. Kawashima, K. Hatada, Chromatographic resolution: XI. Controlled chiral recognition of cellulose triphenylcarbamate derivatives supported on silica gel, J. Chromatogr. A 363 (1986) 173–186.